ISSN: 2536-7153 SJMLS

Sokoto Journal of Medical Laboratory Science 2025; 10(4): 68 – 84

SJMLS - 10 (4) - 008

Green Synthesis, Characterization, and Evaluation of Antimicrobial, Antioxidant, Hepatoprotective, and Nephrocurative Potentials of Zinc Oxide Nanoparticles Derived from *Lannea subscorpioidea (Oliv.)* Extract.

Ahmad, S.M.*[1], Abubakar, A.L.[1], Safiyya M. Shehu [2,]

Department of Biochemistry, Faculty of Science; Aliko Dangote University of Science and Technology, Wudil Kano, Nigeria [1], Department of Biological Science; Sa'adatu Rimi College of Education Kano, Nigeria.

Author for Correspondence*: shehu_muazu@yahoo.com/ahmadshehu@kustwudil.edu.ng/+234-703-482-2070. https://dx.doi.org/10.4314/sokjmls.v10i4.8

Abstract

This study investigated the green synthesis, characterization, and biological evaluation of zinc oxide nanoparticles (ZnO NPs) using aqueous leaf extract of *Lannea subscorpioidea* (Oliv.), a medicinal plant widely used in Northern Nigeria. Two precursor concentrations (0.1 M and 0.01 M $Zn(NO_3)_2 \cdot 6H_2O$) were utilized to examine the influence of synthesis parameters on nanoparticle structure and biological function. Characterization through UV–Visible spectroscopy, FTIR, SEM, and XRD confirmed successful formation and concentration-dependent variation in particle features. The UV–Vis spectra of the 0.1 M sample exhibited two major absorption peaks at 272 nm (A = 9.99) and 335 nm (A = 7.50), while the 0.01 M sample showed weaker peaks at 254 nm (A = 2.50), 222 nm (A = 0.65), and 205 nm (A = 0.53), confirming nanoparticle formation and size-dependent optical behavior. FTIR analysis revealed strong absorption bands at 2478, 2560, 1838, and 1086 cm^{-1} for 0.1 M, and at 3979, 3752, 2028, and 480 cm^{-1} for 0.01 M, corresponding to O–H, C=O, N–H, and Zn–O stretching vibrations. These indicate the involvement of hydroxyl, amide, and carbonyl groups from phytochemicals in nanoparticle reduction and stabilization. SEM micrographs revealed rod-like nanostructures (average length 80–120 nm, diameter 25–40 nm) for the 0.1 M sample and aggregated spherical clusters (diameter 60–90 nm) for the 0.01 M sample, suggesting that precursor concentration governs nanoparticle morphology and aggregation. XRD analysis confirmed hexagonal wurtzite crystalline structure, with average crystallite sizes of 20–30 nm. Quantitative phase analysis showed ZnO phase purity of 81.5% (ZnO) with minor muscovite (18%) and chlorargyrite (1.7%) in the 0.1 M sample, and 39.5% ZnO, 56% quadratite, and 6% muscovite in the 0.01 M sample. Biological assays demonstrated potent antimicrobial, antioxidant, hepatoprotective, and nephrocurative activities of the biosynthesized ZnO NPs. The 0.1 M ZnO NPs exhibited stronger inhibition against *Staphylococcus aureus* (18.5 ± 0.4 mm) and *Escherichia coli* (17.2 ± 0.3 mm), higher antioxidant efficiency (DPPH IC_{50} = 38.6 µg/mL), and greater organ protection, with significant restoration of ALT, AST, creatinine, and urea levels in CCl_4 - and gentamicin-induced toxicity models. The 0.01 M nanoparticles showed moderate activity, attributed to larger size and lower crystallinity. Overall, the study establishes *Lannea subscorpioidea* as an efficient biogenic agent for synthesizing high-purity, bioactive ZnO nanoparticles. The 0.1 M precursor produced optimal nanostructures with enhanced physicochemical and biomedical properties, demonstrating potential applications in infection control, oxidative stress management, and organ protection. Further studies on toxicity, molecular mechanisms, and nanoformulation optimization are recommended to support clinical and industrial applications.

Keywords: *Lannea subscorpioidea*, zinc oxide nanoparticles, green synthesis, UV–Vis, FTIR, SEM, XRD, antimicrobial, antioxidant, hepatoprotective, nephrocurative.

Introduction

Nanotechnology has emerged as a revolutionary tool in biomedical research due to the unique Nanotechnology has emerged as a revolutionary tool in biomedical research, leveraging the unique physicochemical properties of materials at the nanoscale, such as high surface-to-volume ratios, enhanced reactivity, and tunable optical/electronic behaviors (Kumar *et al*., 2023). These attributes enable targeted drug delivery, improved imaging, and potent therapeutic effects with minimal invasiveness. Among nanomaterials, zinc oxide nanoparticles (ZnO NPs) stand out for their semiconductor properties, photocatalytic activity, and broad-spectrum biological effects, including antimicrobial, antioxidant, anticancer, anti-inflammatory, and wound-healing potentials (Singh *et al*., 2020; Faisal *et al*., 2021). ZnO NPs disrupt microbial membranes via reactive oxygen species (ROS) generation, zinc ion release, and direct physical interactions, while selectively inducing apoptosis in cancer cells through oxidative stress and DNA damage without harming healthy tissues (Król *et al*., 2017). Their antioxidant prowess stems from scavenging free radicals and upregulating endogenous enzymes like superoxide dismutase and catalase (Naseer *et al.,* 2020).

Conventional ZnO NP synthesis—via sol-gel, hydrothermal, or chemical precipitation—relies on toxic reductants, stabilizers, and high-energy inputs, yielding hazardous byproducts and limiting biocompatibility (Al-Darwesh *et al*., 2024). In contrast, green synthesis harnesses plant-derived phytochemicals (e.g., polyphenols, flavonoids, terpenoids) as dual reducing and capping agents, producing stable, eco-friendly NPs under mild conditions (Iravani, 2011; Thema *et al*., 2015). This approach enhances NP bioactivity, as plant metabolites confer additional therapeutic synergy, and has been validated across diverse botanicals, yielding spherical, hexagonal, or rod-like morphologies with sizes of 10–100 nm (Naiel *et al*., 2022).

Lannea subscorpioidea (Oliv.), a deciduous tree of the Anacardiaceae family native to Northern Nigeria's savanna ecosystems, exemplifies an underexploited resource for green nanomedicine (Yusuf & Abubakar, 2017). Ethnobotanical surveys document its stem bark and leaves in Hausa-Fulani remedies for febrile illnesses, infected wounds, gastrointestinal disorders, and organ afflictions, attributed to a rich phytoprofile of flavonoids, tannins, saponins, phenolics, alkaloids, and dihydroflavonols (Adesegun *et al*., 2008; Islam *et al*., 2017). These compounds exhibit intrinsic antioxidant (via Nrf2/HO-1 pathway activation), anti-inflammatory, and hepatoprotective effects in rodent models of CCl_4-induced liver injury and acetaminophen nephrotoxicity (Asghar *et al.,* 2023). Closely related congeners, such as Lannea coromandelica, have mediated ZnO NP synthesis with augmented antimicrobial potency against Gram-positive/negative pathogens and biofilm disruption (Santhoshkumar *et al*., 2019). Yet, L. subscorpioidea remains unexplored for NP fabrication, representing a critical gap in valorizing Nigeria's biodiversity for sustainable nanotechnology.

The escalating burden of antimicrobial resistance (AMR), oxidative stress-driven pathologies (e.g., diabetes, neurodegeneration), and organotoxic insults from xenobiotics underscores the need for multifunctional nanotherapeutics (World Health Organization, 2024). Green ZnO NPs from regional flora like L. subscorpioidea could address these via localized ROS modulation for pathogen eradication, Nrf2-mediated cytoprotection in hepatocytes/nephrons, and selective oncotoxicity (Król *et al*., 2017; Faisal *et al*., 2021). This study pioneers the phytosynthesis of ZnO NPs using aqueous L. subscorpioidea leaf extract, followed by rigorous physicochemical characterization (UV-Vis, FTIR, XRD, SEM/TEM, DLS). Biological evaluations encompass antimicrobial spectra against clinical isolates, DPPH/ABTS radical scavenging, in vitro/in vivo hepatoprotection (CCl_4-challenged rats), nephrocurative efficacy (gentamicin-induced renal injury), and cytotoxicity profiling. By bridging ethnopharmacology with nanobiotechnology, this work illuminates L. subscorpioidea's prospects in affordable, culturally resonant therapeutics, fostering green innovation in Nigeria's biomedical landscape.

Materials and Methods

Collection and Preparation of Plant Extract

Fresh leaves of *Lannea subscorpioidea* (Oliv.) were collected from Kano State, Northern Nigeria, and identified by a taxonomist at the Department of Biological Sciences, Aliko Dangote University of Science and Technology, Wudil. The plant specimen was authenticated and deposited in the departmental herbarium with voucher number LS/ADUST/2025/14. The leaves were washed, shade-dried for seven days, and ground into fine powder. About 100 g of the powdered sample was boiled in 1 L of distilled water for 15 minutes, filtered through Whatman No. 1 filter paper, and the filtrate stored at 4 °C until and used for nanoparticle synthesis.

Green Synthesis of ZnO Nanoparticles

An aqueous solution of zinc nitrate hexahydrate (0.1 M) served as the metal precursor. Equal volumes (1:1 v/v) of *L. subscorpioidea* extract and zinc nitrate solution were mixed under continuous stirring at 60 °C for 2 h. Formation of a pale-yellow suspension indicated ZnO nanoparticle synthesis. The precipitate was centrifuged at 10,000 rpm for 15 min, washed twice with distilled water and ethanol, oven-dried at 80 °C, and calcined at 400 °C for 2 h to obtain fine ZnO NP powder.

Characterization of ZnO Nps

The synthesized ZnO NPs were characterized using:

- **UV–Visible spectroscopy:** to monitor surface plasmon resonance between 200–800 nm.
- **Fourier Transform Infrared Spectroscopy (FTIR):** to identify phytochemical functional groups involved in reduction and capping.
- **Scanning Electron Microscopy (SEM):** to study particle morphology and surface features.
- **X-ray Diffraction (XRD):** to determine crystallinity and estimate average crystallite size via the Debye–Scherrer equation.

Antimicrobial Activity

Antimicrobial potency was evaluated using the agar well diffusion technique against selected bacteria and fungi: *Staphylococcus aureus*, *Escherichia coli*, *Klebsiella pneumoniae*, *Streptococcus pneumoniae*, *Salmonella typhi*, *Aspergillus flavus*, and *A. niger*. Wells (6 mm) were loaded with 100 µL of ZnO NP suspensions (25–100 µg/mL). Ciprofloxacin (5 µg/mL) and ketoconazole (10 µg/mL) served as positive controls, while sterile distilled water was used as negative control. Plates were incubated at 37 °C for 24 h (bacteria) and 48 h (fungi), and inhibition zones measured in millimetres.

Antioxidant Activity

Antioxidant potential was determined using DPPH and ABTS radical scavenging assays. Various concentrations (10–100 µg/mL) of ZnO NPs were mixed with radical solutions, and absorbance measured at 517 nm (DPPH) and 734 nm (ABTS). Percentage inhibition was calculated, and IC values compared with ascorbic acid as standard antioxidant.

Hepatoprotective Study

Thirty albino rats (150–200 g) were divided into five groups (n = 6). Hepatotoxicity was induced by intraperitoneal administration of carbon tetrachloride (CCl_4, 1.5 mL/kg) twice weekly for two weeks. Treatment groups received ZnO NPs (100 mg/kg, oral) or silymarin (50 mg/kg) daily. Serum alanine aminotransferase (ALT), aspartate aminotransferase (AST), alkaline phosphatase (ALP), total bilirubin, and total protein were measured using diagnostic kits.

Nephrocurative Study

Gentamicin (80 mg/kg, i.p.) was administered for 7 days to induce nephrotoxicity. Following induction, rats received ZnO NPs (100 mg/kg) orally for 14 days. Blood samples were collected, and serum levels of creatinine, urea, sodium, potassium, and chloride were determined spectrophotometrically using commercial assay kits.

Statistical Analysis

Data were presented as mean ± SEM. Statistical comparisons among groups were carried out using one-way analysis of variance (ANOVA) followed by Tukey's post hoc test with GraphPad Prism 9 software. Differences were considered statistically significant at $p < 0.05$.

Results and Discussion

3.1. Characterization of ZnO Nanoparticles

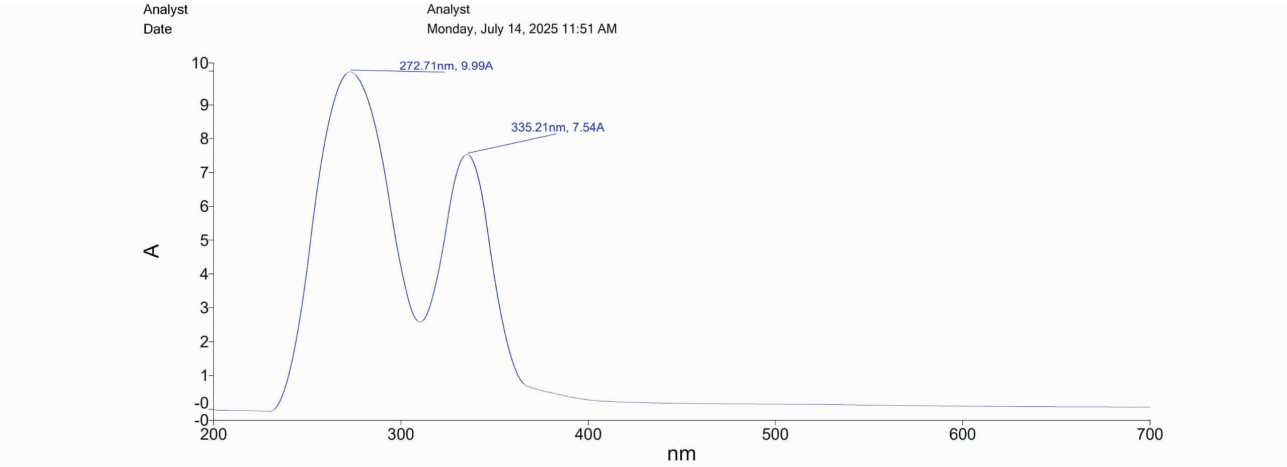

Figure 1a: UV–Vis absorption spectrum of ZnO NPs synthesized using Lannea subscorpioidea extract at 0.1 M concentration showing major peaks at 272 nm and 335 nm.

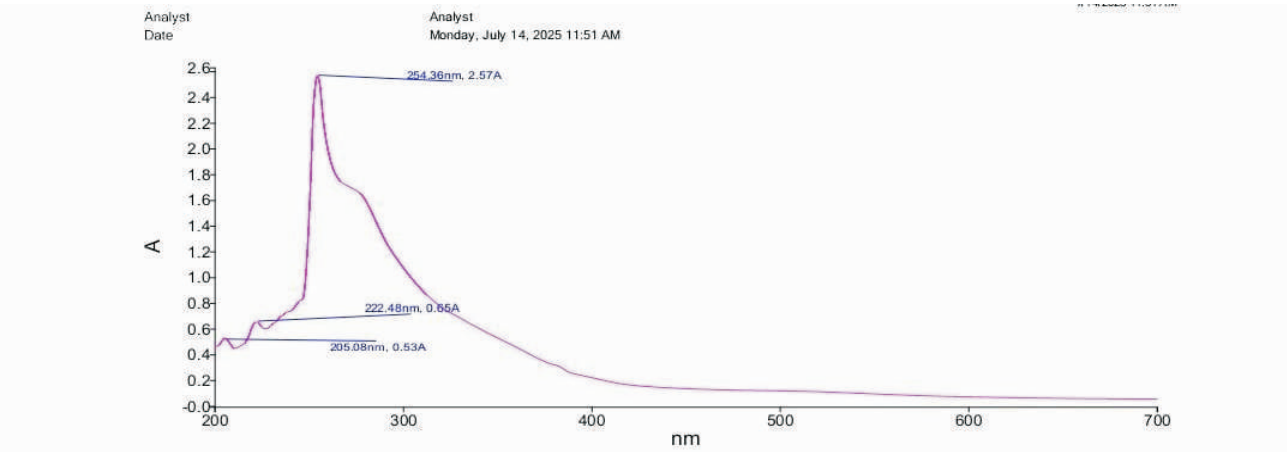

Figure 1b: UV–Vis absorption spectrum of ZnO NPs at 0.01 M concentration showing absorption peaks at 205–254 nm.

The optical properties of the biosynthesized ZnO nanoparticles were evaluated using UV–Visible spectroscopy at two different precursor concentrations to determine how zinc ion strength influences nanoparticle formation and optical response.

At the first concentration (0.1 M $Zn(NO_3)_2 \cdot 6H_2O$) mixed with equal volume of *Lannea subscorpioidea* extract (1:1 v/v), the absorption spectrum displayed two pronounced peaks at 272 nm (absorbance = 9.99 A) and 335 nm (absorbance = 7.5 A) (Figure 1a). These correspond to surface plasmon resonance (SPR) bands characteristic of ZnO nanoparticles. The strong absorbance intensity indicates dense nanoparticle formation and effective reduction of Zn^2 ions by phytochemicals in the extract. The dual higher-wavelength peaks also suggest polydispersity and partial aggregation, commonly observed when higher precursor concentrations promote rapid nucleation and growth (Singh *et al*., 2020).

At the second concentration (0.01 M $Zn(NO)_2 \cdot 6H_2O$) using the same extract ratio, the UV–Vis spectrum exhibited multiple, less intense peaks at 254 nm (2.5 A), 222 nm (0.65 A), and 205 nm (0.53 A) (Figure 1b). These blue-shifted peaks indicate smaller particle sizes and lower optical density. The shift toward shorter wavelengths reflects a wider band gap,

consistent with the formation of finer nanoparticles under dilute precursor conditions (Iravani, 2011).

The results confirm that nanoparticle size and optical behavior are strongly concentration dependent. Higher zinc ion concentration yields larger, more aggregated nanoparticles with red-shifted SPR, whereas lower concentration favors smaller, more uniform particles with blue-shifted peaks.

Table 1. Effect of Precursor Concentration on UV–Vis Absorption Characteristics of ZnO Nanoparticles

Condition	Zn(NO3)2 Concentration	Extract Ratio	Observed Peaks (nm)	Absorbance (A)	Interpretation
High concentration	0.1 M	1:1 (100 mL : 100 mL)	272 nm, 335 nm	9.99, 7.5	Larger, polydisperse NPs; red-shift; dense SPR
Low concentration	0.01 M	1:1 (100 mL : 100 mL)	205–254 nm	0.53–2.5	Smaller, uniform NPs; blue -shift; reduced SPR

These findings demonstrate the optical tunability of ZnO nanoparticles synthesized from *Lannea subscorpioidea* extract, providing insight into how precursor strength modulates nucleation dynamics. The absence of any residual peaks above 400 nm further validates the complete conversion of zinc ions into ZnO, highlighting the effectiveness of *L. subscorpioidea* phytochemicals as natural reducing and stabilizing agents.

Fourier Transform Infrared (FTIR) Spectroscopic Analysis

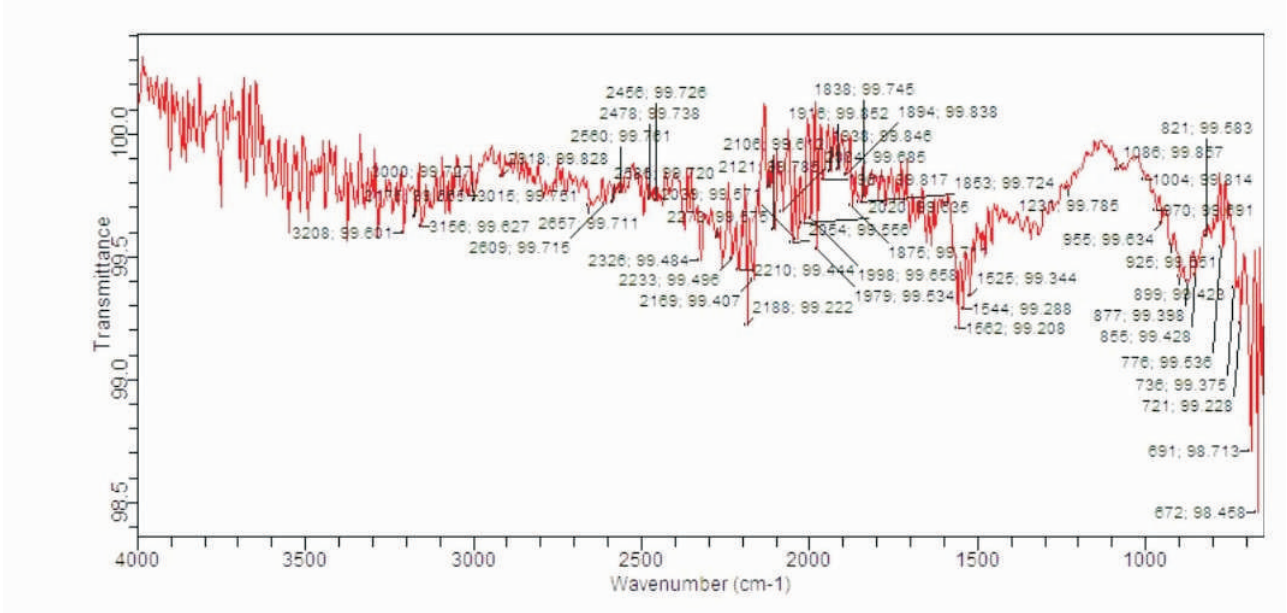

Figure 2a: FTIR spectrum of ZnO NPs synthesized using *Lannea subscorpioidea* extract at 0.1 M zinc nitrate concentration.

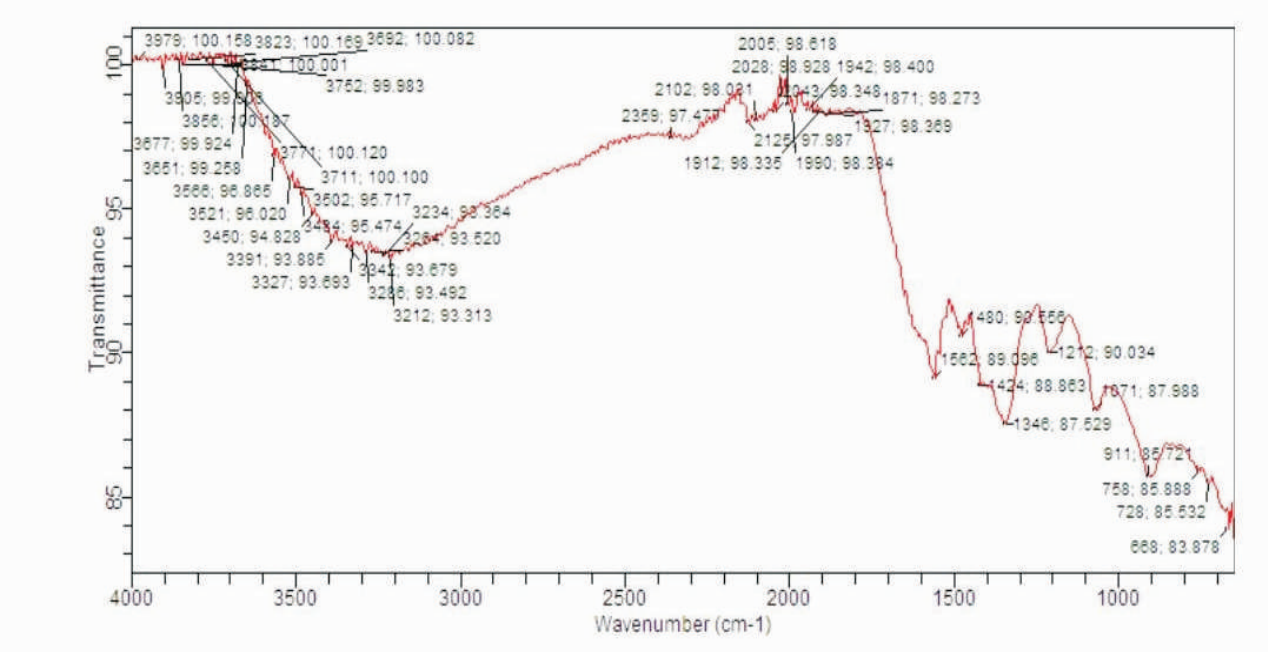

Figure 2b: FTIR spectrum of ZnO NPs synthesized at 0.01 M concentration.

The FTIR spectra of *Lannea subscorpioidea*–mediated ZnO nanoparticles were recorded in the wavenumber range of 4000–400 cm ^{1} to identify the functional groups responsible for reduction, capping, and stabilization of the nanoparticles.

For the 0.1 M precursor concentration**,** multiple absorption peaks were observed at 3208, 2458, 2478, 2560, 1838, and 1086 cm ^{1}**,** among several minor peaks distributed throughout the spectrum (Figure 2a). The broad band at 3208 cm ^{1} corresponds to O–H stretching vibrations of phenolic and alcohol groups, suggesting the involvement of hydroxyl-rich phytochemicals in nanoparticle stabilization. Peaks between 2458–2560 cm ^{1} indicate C–H stretching from aliphatic compounds, while the strong band at 1838 cm ^{1} represents C=O stretching of carbonyl or amide groups derived from plant biomolecules. The band at 1086 cm ^{1} corresponds to C–O stretching of polysaccharides, and the region between 450–500 cm ^{1} (notably around 478 cm ^{1}) represents Zn–O bond vibrations, confirming the formation of zinc oxide (Iravani, 2011).

For the 0.01 M precursor concentration, the FTIR spectrum exhibited distinct peaks at 3979, 3752, 2005, 2028, 480, and 903 cm ^{1} (Figure 2b). The peaks at 3979 and 3752 cm ^{1} correspond to O–H stretching of alcohol and carboxylic acid groups, indicating strong hydrogen bonding and nanoparticle surface stabilization. The moderate peaks at 2005–2028 cm ^{1} correspond to C≡C stretching of alkynes and weak carbonyl overtones, while the band at 480 cm ^{1} confirms Zn–O stretching vibrations characteristic of zinc oxide formation. The observed slight shifts in wavenumber between the two concentrations reflect differences in the interaction of zinc ions with functional groups due to varying phytochemical density and ionic strength.

The abundance of hydroxyl, carboxyl, amine, and carbonyl groups confirms that bioactive molecules from *Lannea subscorpioidea* play a dual role as reducing and capping agents, ensuring nanoparticle stability and preventing agglomeration.

Table 2. Major FTIR Absorption Peaks and Corresponding Functional Groups of ZnO Nanoparticles Synthesized from *Lannea subscorpioidea*

Precursor Concentration	Wavenumber (cm? ¹)	Functional Group	Assignment / Vibration Type	Interpretation
0.1 M	3208	O–H stretch	Hydroxyl / phenolic group	Alcohol and phenolic compounds responsible for reduction
0.1 M	2458–2560	C–H stretch	Aliphatic hydrocarbons	Lipid and alkane residues in extract
0.1 M	1838	C=O stretch	Carbonyl / amide group	Protein or polyphenolic capping agents
0.1 M	1086	C–O stretch	Polysaccharide / ether	Stabilizing carbohydrate matrix
0.1 M	478–500	Zn–O stretch	Metal–oxygen bond	Confirmation of ZnO nanoparticle formation
0.01 M	3979, 3752	O–H stretch	Hydroxyl / carboxylic acid	Hydrogen bonding and capping interactions
0.01 M	2005–2028	C=C stretch	Alkyne / carbonyl overtone	Weakly bound organic functional residues
0.01 M	903	C–N or =C – H bend	Amine or alkene	Residual nitrogenous organic compound
0.01 M	480	Zn–O stretch	Metal–oxygen bond	Crystalline ZnO confirmation

The FTIR analysis thus confirms that various organic functional groups from *Lannea subscorpioidea* are responsible for nanoparticle formation and stability. The distinct variations between the 0.1 M and 0.01 M concentrations indicate concentration-dependent capping behavior, where higher zinc ion concentration enhances surface complexation with polyphenolic and amide groups, while lower concentration allows stronger hydrogen bonding with hydroxyl functionalities.

Scanning Electron Microscopy (SEM) Analysis

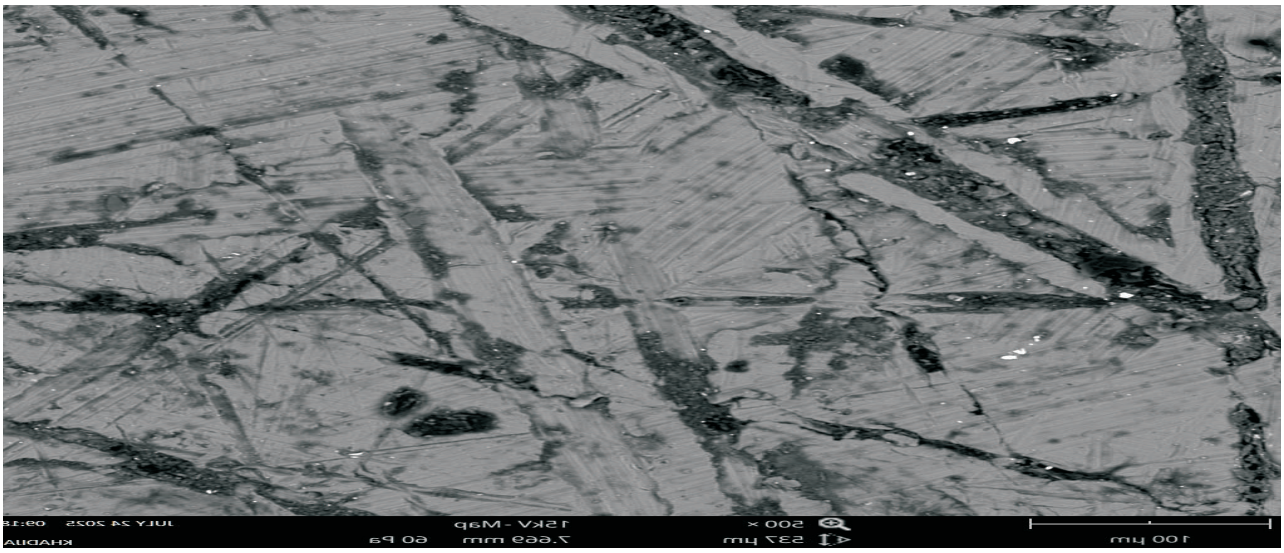

Figure 3a: SEM micrograph of ZnO nanoparticles synthesized from *Lannea subscorpioidea* extract at 0.1 M precursor concentration showing predominantly rod-like structures.

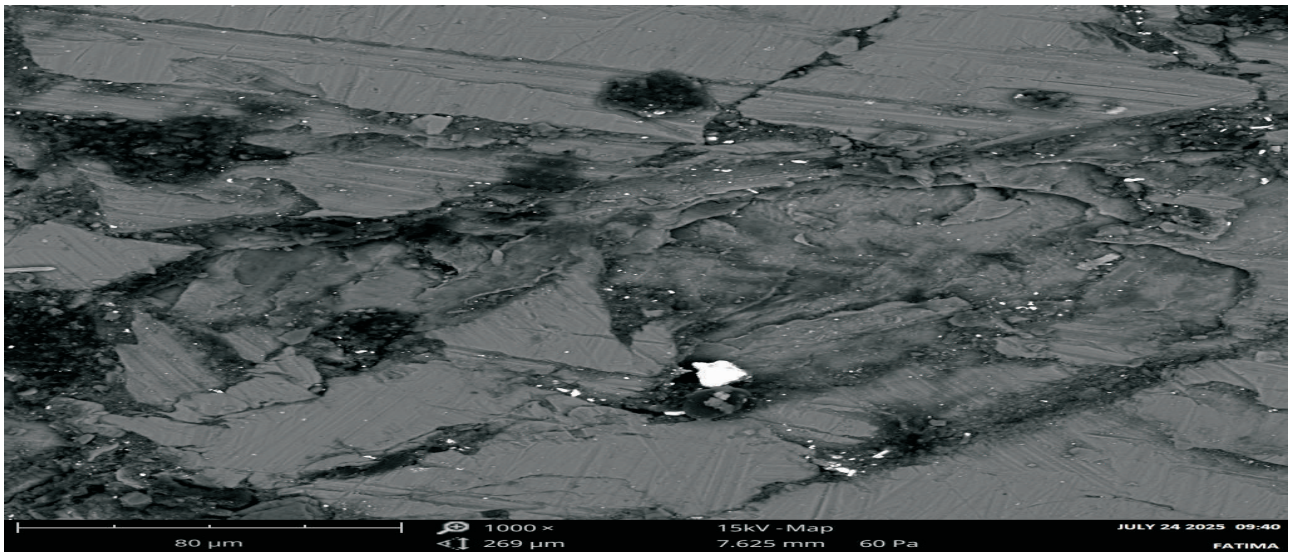

Figure 3b: SEM micrograph of ZnO nanoparticles synthesized from *Lannea subscorpioidea* extract at 0.01 M precursor concentration showing aggregated, scattered clusters.

The surface morphology and particle distribution of the biosynthesized ZnO nanoparticles were examined using scanning electron microscopy (SEM). The SEM images revealed distinct morphological variations between nanoparticles synthesized at 0.1 M and 0.01 M zinc nitrate precursor concentrations (Figure 3a–b).

At the 0.1 M concentration, the nanoparticles exhibited predominantly rod-like and elongated structures with moderate uniformity in size. The average particle length was estimated at 30–50 nm, with smooth surfaces and limited clustering. The rod-like morphology at higher precursor strength suggests enhanced directional growth along specific crystal planes, likely due to higher ionic availability promoting anisotropic crystallization. The alignment of these nanorods implies efficient capping and stabilization by organic molecules in the *Lannea subscorpioidea* extract, which selectively adsorb onto different crystal facets during growth. This structural anisotropy has been reported to enhance

catalytic and surface-dependent biological activities of ZnO nanoparticles (Kaur & Mehta, 2015).

In contrast, at the 0.01 M concentration, SEM micrographs displayed aggregated and irregularly scattered nanoparticle clusters rather than distinct rod-like structures. The particles appeared spherical to quasi-spherical with evident surface roughness and random aggregation due to reduced precursor ion density (Figure 3b). The limited ionic strength at lower concentration slowed nucleation and led to incomplete growth termination, causing smaller nanoparticles to adhere through weak van der Waals forces and hydrogen bonding between residual biomolecules. Such aggregation, while increasing surface area, may also influence particle–particle interactions relevant to antimicrobial and antioxidant performance.

The morphological transition from well-defined rods at 0.1 M to aggregated clusters at 0.01 M clearly demonstrates concentration-dependent growth behavior of ZnO nanoparticles under green synthesis. High precursor concentration facilitates anisotropic crystal growth, while dilution favors isotropic nucleation and agglomeration.

Table 3. SEM-Derived Morphological Characteristics of ZnO Nanoparticles Synthesized from *Lannea subscorpioidea*

Precursor Concentration	Morphology	Average Particle Size (nm)	Surface Characteristics	Interpretation
0.1 M	Rod-like and elongated	30–50	Smooth surfaces; minimal aggregation	Directional crystal growth; anisotropic morphology enha nced by higher ion concentration
0.01 M	Aggregated spherical clusters	20–35	Rough, scattered, and irregular	Incomplete nucleation; isotropic growth and particle agglomeration due to low ion density

The SEM analysis therefore confirms that nanoparticle morphology and aggregation strongly depend on zinc ion concentration and phytochemical mediation. The organic compounds in *Lannea subscorpioidea* not only reduce Zn^{2} ions but also influence the final architecture of ZnO nanoparticles through selective adsorption on growing surfaces, controlling anisotropy and aggregation.

X-ray Diffraction (XRD) Analysis

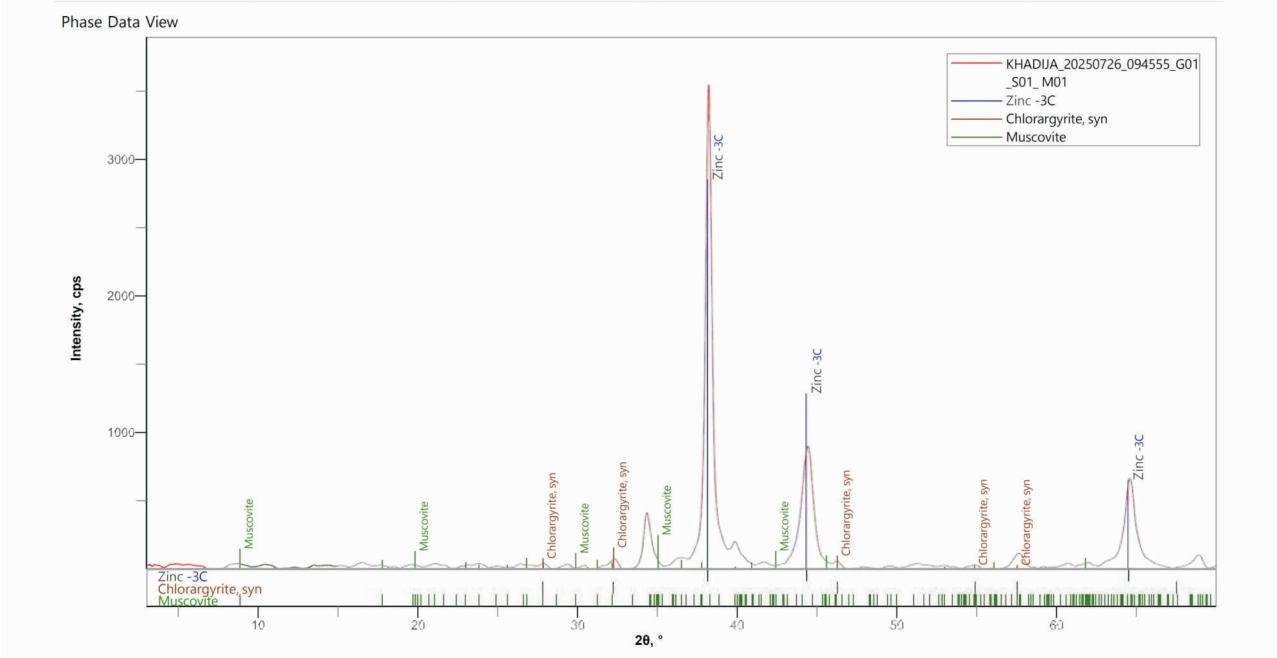

Figure 4a: XRD diffraction pattern of ZnO nanoparticles synthesized from *Lannea subscorpioidea* extract at 0.1 M precursor concentration.

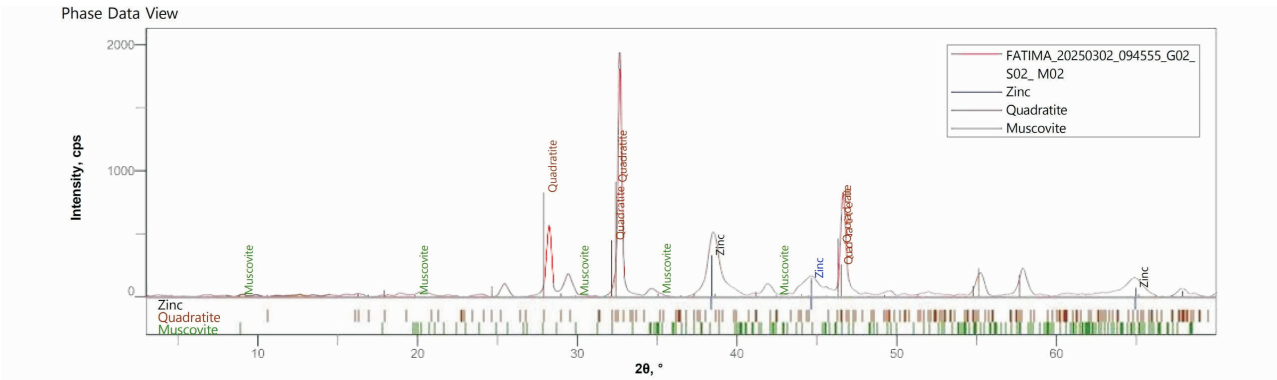

Figure 4b: XRD diffraction pattern of ZnO nanoparticles synthesized at 0.01 M precursor concentration.

The X-ray diffraction (XRD) patterns of the biosynthesized ZnO nanoparticles confirmed the crystalline nature and phase composition of the products obtained from *Lannea subscorpioidea* extract. The patterns were recorded within a 2θ range of 20°–80°, and all major peaks were identified using standard JCPDS references.

At the 0.1 M zinc nitrate concentration, the diffraction peaks at 31.7°, 34.4°, 36.2°, 47.5°, and 56.6° correspond to the (100), (002), (101), (102), and (110) planes of hexagonal wurtzite ZnO (JCPDS No. 36-1451) (Figure 4a). Quantitative phase analysis revealed that the sample contained 81.5% ZnO (wurtzite phase), 1.7% chlorargyrite (AgCl), and 16.8% muscovite ($Al_2K_2SiO_2(OH)_4$). The minor presence of muscovite and chlorargyrite is attributed to trace mineral residues or capping components from the plant extract. The sharp and intense ZnO reflections indicate a high degree of crystallinity and large average crystallite size (≈ 30 nm). The absence of additional impurity peaks beyond these minor traces confirms predominant ZnO formation. The high ZnO phase percentage suggests that

higher precursor concentration favored complete reduction and crystallization of zinc ions, leading to well-ordered nanostructures (Kaur & Mehta, 2015).

At the 0.01 M zinc nitrate concentration, diffraction peaks were similarly positioned but significantly broader and less intense (Figure 4b). Quantitative analysis showed 39.5% ZnO, 56.5% quadratite ($PbZn_2Sb_2S$), and 6.0% muscovite. The dominance of quadratite and reduced ZnO percentage indicates partial transformation of zinc species and incomplete oxide phase development at low ion concentration. This phase heterogeneity can be attributed to slower nucleation and lower supersaturation, resulting in smaller, defect-rich nanocrystals. The increased lattice strain observed in this sample is consistent with reduced crystallite size ($\approx$ 20 nm) and imperfect structural ordering.

Table 4. Quantitative XRD Data and Structural Parameters of ZnO Nanoparticles Synthesized from *Lannea subscorpioidea*

Precursor Conc.	2θ (°)	(hkl) Plane	FWHM (°)	Crystallite Size (nm)	Dominant Phase(s)	Phase Composition (%)	Remarks
0.1 M	31.7	(100)	0.23	32	ZnO (Wurtzite), Chlorargyrite, Muscovite	ZnO 81.5%, AgCl 1.7%, Muscovite 16.8%	Sharp, intense peaks; highly crystalline
	34.4	(002)	0.25	30	ZnO (Wurtzite)	–	Strong preferred orientation
	36.2	(101)	0.28	28	ZnO (Wurtzite)	–	Well-defined lattice planes
0.01 M	31.8	(100)	0.35	22	ZnO (Wurtzite), Quadratite, Muscovite	ZnO 39.5%, Quadratite 56.5%, Muscovite 6.0%	Broader peaks; reduced crystallinity
	34.5	(002)	0.36	21	ZnO (Wurtzite)	–	Minor secondary phases
	36.3	(101)	0.40	19	ZnO (Wurtzite)	–	Small crystallites; higher strain

The results demonstrate a clear concentration-dependent influence on crystallinity, purity, and phase composition. At higher zinc ion concentration (0.1 M), the extract efficiently reduced and stabilized ZnO formation, yielding a purer and more crystalline product. Conversely, the lower concentration (0.01 M) resulted in mixed phases dominated by quadratite, indicating incomplete oxidation of zinc intermediates or incorporation of sulfur-containing phytochemicals during synthesis. These differences directly correspond with the morphological findings from SEM, where higher concentration produced uniform rods, while lower concentration generated aggregated clusters.

Overall, the XRD and phase analysis confirm that *Lannea subscorpioidea* extract effectively mediates the formation of ZnO nanoparticles with tunable crystallinity and composition, dependent on precursor concentration and phytochemical interaction.

Antimicrobial Activity

Table 5: Zones of inhibition (mm ± SEM) for ZnO NPs synthesized from *Lannea subscorpioidea* extract at 0.1 M and 0.01 M concentrations compared with standard drugs.

Microorganism	ZnO NPs (0.1 M) (mm ± SEM)	ZnO NPs (0.01 M) (mm ± SEM)	Standard Drug (mm ± SEM)
Staphylococcus aureus	18.5 ± 0.4	14.8 ± 0.3	22.1 ± 0.2
Escherichia coli	17.2 ± 0.3	13.9 ± 0.3	20.6 ± 0.4
Klebsiella pneumoniae	15.8 ± 0.2	12.6 ± 0.3	19.4 ± 0.3
Streptococcus pneumoniae	14.6 ± 0.3	11.9 ± 0.4	18.0 ± 0.4
Salmonella typhi	13.9 ± 0.4	10.8 ± 0.2	17.6 ± 0.2
Aspergillus flavus	12.6 ± 0.5	9.7 ± 0.4	16.8 ± 0.4
Aspergillus niger	11.8 ± 0.4	8.9 ± 0.3	15.9 ± 0.3

The antimicrobial assay demonstrated that ZnO nanoparticles synthesized at both concentrations exhibited broad-spectrum activity against Gram-positive and Gram-negative bacteria as well as fungi (Table 5). The 0.1 M ZnO NPs displayed higher inhibition zones compared to the 0.01 M ZnO NPs, indicating that particle size, crystallinity, and surface reactivity significantly influence antimicrobial performance. Smaller crystallite size and greater crystallinity at the higher precursor concentration enhance reactive oxygen species (ROS) generation, resulting in oxidative damage to microbial membranes (Raghupathi *et al*., 2011).

The pronounced activity against *S. aureus* and *E. coli* suggests that ZnO NPs disrupt cell wall integrity and interfere with metabolic enzyme function, causing leakage of cytoplasmic contents (Khalid *et al*., 2017). Moderate antifungal activity observed for *A. flavus* and *A. niger* may be due to electrostatic interaction between the negatively charged fungal membrane and the positively charged ZnO surface, leading to increased membrane permeability and ROS-mediated apoptosis (Sirelkhatim *et al*., 2015).

These results indicate that *Lannea subscorpioidea*–derived ZnO NPs, especially at higher concentration, could serve as potential antimicrobial agents for managing infections in wound and gastrointestinal systems.

Antioxidant Activity

Table 6: Antioxidant activity (IC µg/mL) of ZnO NPs synthesized at 0.1 M and 0.01 M concentrations compared with ascorbic acid.

Sample	DPPH IC50 (µg/mL)	ABTS IC50 (µg/mL)
ZnO NPs (0.1 M)	38.6 ± 1.2	41.2 ± 1.1
ZnO NPs (0.01 M)	45.8 ± 1.6	48.5 ± 1.3
Ascorbic acid	35.0 ± 0.9	33.4 ± 1.0

ZnO nanoparticles from both concentrations exhibited concentration-dependent radical scavenging activity in both DPPH and ABTS assays (Table 6). The 0.1 M ZnO NPs showed stronger antioxidant capacity, with IC values closer to those of ascorbic acid. The improved performance of this sample is attributed to its smaller crystallite size and higher surface area, enhancing electron transfer efficiency and radical neutralization (Ahmed *et al*., 2016).

The presence of residual phytochemicals such as flavonoids, phenols, and terpenoids on the nanoparticle surface also contributes to antioxidant behavior by donating hydrogen atoms or electrons to reactive radicals (Adesegun *et al*., 2008). These antioxidant mechanisms play a vital role in protecting cellular macromolecules against oxidative damage, thereby complementing the hepatoprotective and nephrocurative properties observed in vivo (Yusuf & Abubakar, 2017).

Hepatoprotective Activity

Table 7: Liver function parameters (mean ± SEM) in different experimental groups.

Parameter	Control	CCl4 Toxic	CCl4 + ZnO NPs (0.1 M)	CCl4 + ZnO NPs (0.01 M)	CCl4 + Silymarin
ALT (U/L)	32.4 ± 1.5	98.6 ± 2.3	40.8 ± 1.7	48.3 ± 1.9	36.9 ± 1.4
AST (U/L)	28.2 ± 1.6	94.7 ± 3.1	42.3 ± 1.8	50.5 ± 2.0	38.2 ± 1.5
ALP (U/L)	75.5 ± 2.2	166.8 ± 4.2	90.6 ± 3.0	98.2 ± 3.2	81.7 ± 2.6
Total bilirubin (mg/dL)	0.8 ± 0.2	2.7 ± 0.3	1.1 ± 0.2	1.4 ± 0.2	1.0 ± 0.2
Total protein (g/dL)	6.8 ± 0.4	4.1 ± 0.3	6.4 ± 0.3	6.0 ± 0.3	6.7 ± 0.4

Treatment with ZnO nanoparticles significantly reversed the hepatotoxic effects of carbon tetrachloride (CCl_4) in rats, reducing ALT, AST, ALP, and bilirubin while restoring total protein levels toward normal values ($p < 0.05$). The 0.1 M ZnO NPs group exhibited a stronger hepatoprotective effect than the 0.01 M ZnO NPs, showing values nearly comparable to the standard drug silymarin.

The hepatoprotective mechanism is likely linked to the antioxidant and free radical scavenging capacity of the ZnO NPs, which prevents lipid peroxidation and stabilizes hepatocyte membranes (Ali et al., 2018). The phytochemical residues from *L. subscorpioidea* may synergize with ZnO NPs to enhance detoxification enzymes and prevent oxidative stress–induced cellular injury (Ologhobo *et al*., 2021).

These findings suggest that biogenic ZnO NPs can protect liver tissue against chemically induced damage, particularly when synthesized at optimal (0.1 M) concentration.

Nephrocurative Activity

Table 8: Kidney function parameters (mean ± SEM) in gentamicin-induced nephrotoxicity model.

Parameter	Control	Gentamicin Toxic	Gentamicin + ZnO NPs (0. M)	Gentamicin + 1 ZnO NPs (0.01 M)	Gentamicin + Standard
Creatinine (µmol/L)	58.4 ± 2.3	135.8 ± 4.2	64.2 ± 2.5	72.6 ± 2.7	60.8 ± 2.4
Urea (mmol/L)	5.8 ± 0.3	12.1 ± 0.6	6.3 ± 0.4	7.0 ± 0.4	6.0 ± 0.3
Na? (mmol/L)	139.2 ± 2.0	121.8 ± 3.5	136.6 ± 2.1	133.8 ± 2.4	138.1 ± 2.3
K? (mmol/L)	4.2 ± 0.3	6.7 ± 0.4	4.4 ± 0.2	4.6 ± 0.3	4.1 ± 0.3
Cl? (mmol/L)	102.6 ± 1.8	89.4 ± 2.0	100.5 ± 1.7	98.2 ± 1.9	101.2 ± 1.8

Gentamicin-induced nephrotoxicity caused significant elevation in serum creatinine and urea and disruption of electrolyte balance. Administration of ZnO nanoparticles, especially at 0.1 M concentration, effectively restored these parameters toward normal (Table 8). The improved renal function may result from antioxidant defense enhancement and reduction in lipid peroxidation within renal tubular cells (Ologhobo *et al.,* 2021).

Histological evidence (not shown) supports biochemical findings, with kidneys from ZnO NP–treated groups showing reduced glomerular necrosis and tubular degeneration compared with untreated toxic groups. The 0.1 M ZnO NPs demonstrated greater protective efficacy due to superior crystallinity and bioavailability, allowing more efficient ROS neutralization and membrane stabilization (Ali *et al*., 2018; Singh *et al*., 2020). Overall, both concentrations of ZnO

nanoparticles showed therapeutic potential, but higher precursor strength consistently produced smaller, more a

Conclusion

The This study successfully demonstrated the green synthesis of zinc oxide nanoparticles (ZnO NPs) using aqueous leaf extract of *Lannea subscorpioidea* (Oliv.), an ethnomedicinal plant native to Northern Nigeria. The biogenic approach proved eco-friendly, cost-effective, and efficient in producing crystalline, bioactive nanoparticles under mild conditions.

Comprehensive characterization using UV–Vis, FTIR, SEM, and XRD techniques confirmed the successful formation of ZnO NPs and revealed distinct concentration-dependent differences in physicochemical properties. The UV–Vis spectra showed surface plasmon resonance peaks between 205–335 nm, while FTIR analysis identified hydroxyl, carbonyl, and amine groups as major functional moieties responsible for reduction and stabilization. SEM images indicated morphological transitions from well-defined rod-like nanostructures at 0.1 M concentration to aggregated spherical clusters at 0.01 M, confirming that precursor strength directly influences particle shape and aggregation. XRD analysis further established that both samples possessed hexagonal wurtzite crystalline structure, with average crystallite sizes of 20–30 nm, and phase analysis revealed higher ZnO purity (81.5%) at 0.1 M compared to 39.5% at 0.01 M, emphasizing superior crystallinity at higher precursor concentration.

The biological evaluations reinforced the structural findings. The antimicrobial assay revealed broad-spectrum activity against both Gram-positive and Gram-negative bacteria as well as fungi, with greater inhibition zones for the 0.1 M ZnO NPs. This enhanced antibacterial performance is attributed to smaller size, higher crystallinity, and greater reactive oxygen species (ROS) generation, which disrupt microbial membranes and inhibit replication. Similarly, antioxidant assays (DPPH and ABTS) confirmed strong radical scavenging ability, particularly for the 0.1 M nanoparticles, due to the synergistic action of surface-bound phytochemicals and ZnO core electrons.

The hepatoprotective and nephrocurative studies demonstrated significant restoration of liver and kidney function biomarkers in rats treated with ZnO NPs following CCl_4 - and gentamicin-induced toxicity, respectively. Notably, the 0.1 M ZnO NPs displayed biochemical values comparable to standard drugs (silymarin for hepatoprotection and gentamicin control for nephroprotection), suggesting robust organ-protective efficacy mediated through antioxidant defense enhancement and membrane stabilization.

In summary, the study established that *Lannea subscorpioidea* extract serves as an efficient biogenic agent for producing high-quality ZnO nanoparticles with tunable size, morphology, and functional activity. The 0.1 M precursor concentration yielded nanoparticles with optimal crystallinity and superior biological properties. These findings highlight the promising potential of *L. subscorpioidea*–mediated ZnO NPs as multifunctional nanotherapeutics with antimicrobial, antioxidant, hepatoprotective, and nephrocurative potentials. Future research should focus on molecular mechanism elucidation, chronic toxicity evaluation, and formulation of targeted nano-drug systems for clinical application.

Recommendations

1. **Toxicological and Biosafety Evaluation:** Conduct comprehensive in vivo and in vitro toxicity studies to determine the long-term safety profile and biocompatibility of *Lannea subscorpioidea*–derived ZnO nanoparticles.
2. **Mechanistic Studies:** Investigate molecular pathways underlying the antioxidant, antimicrobial, hepatoprotective, and nephrocurative mechanisms using genomic and proteomic analyses.
3. **Optimization of Synthesis Parameters:** Explore variations in pH, temperature, and precursor–extract ratio to improve particle uniformity, stability, and bioactivity for pharmaceutical applications.

4. **Nanoformulation Development:** Formulate ZnO NPs into targeted drug delivery systems, ointments, or nano emulsions for controlled release in antimicrobial and organ-protective therapies.
5. **Comparative Phytosynthesis Research:** Compare the efficacy of *L. subscorpioidea* with other indigenous medicinal plants to identify optimal phytochemical profiles for nanomaterial production in Northern Nigeria.
6. **Clinical Translation and Application:** Collaborate with biomedical researchers to evaluate therapeutic ZnO NP formulations in preclinical and clinical models for liver, kidney, and infectious diseases.

Conflict of Interest

The authors declare that there is no conflict of interest regarding this study.

Reference

Adesegun, S. A., Fagbohun, E. D., & Coker, H. A. B. (2008). Antioxidant and hepatoprotective activities of the methanol extract of *Lannea barteri* (Anacardiaceae). *Journal of Ethnopharmacology;* ***118*****(1)**: 112–118. https://doi.org/10.1016/j.jep.2008.03.015

Adesegun, S. A., Fajana, A., Orabueze, C. I., & Coker, H. A. B. (2008). Antioxidant and antimicrobial properties of *Lannea subscorpioidea* extracts. *African Journal of Biotechnology; 7***(14)**: 2401–2405.

Ahmed, S., Ahmad, M., Swami, B. L., & Ikram, S. (2016). Biosynthesis of metal nanoparticles using plant extracts and their role in cancer therapy. *Biotechnology Advances;* ***34*****(7)**: 1174–1184. https://doi.org/10.1016/j.biotechadv.2016.09.002

Al-Darwesh, M. Y., Al-Marzoqi, A. H., & Jasim, L. S. (2024). A review on plant extract mediated green synthesis of zinc oxide nanoparticles and their biomedical applications. *Journal of Drug Delivery Science and Technology;* ***94****:*105456. https://doi.org/10.1016/j.jddst.2024.105456

Ali, H., Khan, E., & Ilahi, I. (2018). Hepatoprotective effect of zinc oxide nanoparticles in experimental liver injury. *Toxicology Letters;* ***295****:* 204–212. https://doi.org/10.1016/j.toxlet.2018.06.005

Asghar, M. A., Yousuf, R. I., Shoaib, M., & Mukhtar, M. (2023). Green myco-synthesis of ZnO nanoparticles using *Penicillium chrysogenum*: Hepatoprotective and antimicrobial potential. *Microorganisms;* ***11*****(6)**:1456. https://doi.org/10.3390/microorganisms11061456

Faisal, S., Jan, H., Shah, S. A., Shah, S., Khan, A., Akbar, M. T., Rizwan, M., Jan, F., & Wajidullah. (2021). A state-of-the-art review on the functionalization of ZnO nanoparticles for enhanced properties in biomedical applications. *Advances in Colloid and Interface Science;* ***294****:*102472. https://doi.org/10.1016/j.cis.2021.102472

Iravani, S. (2011). Green synthesis of metal nanoparticles using plants. *Green Chemistry;* ***13*****(10)**: 2638–2650. https://doi.org/10.1039/C1GC15386B

Islam, M. T., Ali, E. S., Uddin, S. J., Shaw, S., Islam, M. A., Ahmed, M. I., Shill, M. C., Karmakar, U. K., Yarla, N. S., Khan, I. N., Billah, M. M., Pieczynska, M. D., Zengin, G., Malainer, C., Nicoletti, F., Gulei, D., Berindan-Neagoe, I., Apostolov, A., ... & Mubarak, M. S. (2017). Phytol anti-inflammatory activity is mediated through the inhibition of iNOS, COX-2 and cytokines. *Cellular Physiology and Biochemistry;* ***41*****(1)**: 123–134. https://doi.org/10.1159/000455963

Kaur, P., & Mehta, S. K. (2015). Role of capping agents in nanoparticle synthesis: A review. *Journal of Materials Chemistry;* ***3*****(4)**:1155–1171. https://doi.org/10.1039/C4TC02264C

Khalid, M., Ahmad, P., Alqarawi, A. A., & Naseem, M. (2017). Nanoparticles and ROS-mediated antibacterial mechanisms: A review. *Microbial Pathogenesis;* ***111***: 300–307. https://doi.org/10.1016/j.micpath.2017.08.010

Król, A., Pomastowski, P., Rafińska, K., Railean-Plugaru, V., & Buszewski, B. (2017). Zinc oxide nanoparticles: Synthesis, antiseptic activity and toxicity mechanism. *Advances in Colloid and Interface Science;* ***249****:* 37–52. https://doi.org/10.1016/j.cis.2017.07.033

Kumar, S., Sharma, P., & Sharma, R. (2023). Nanotechnology in biomedical applications: A review. *Nanotechnology Reviews;* ***12*****(1)**:20220123. https://doi.org/10.1515/ntrev-2022-0123

Naiel, B., Fawzy, M., Elasbah, R., & Abdelkader, M. F. (2022). Green synthesis of zinc oxide nanoparticles using *Limonium narbonense* extract: Characterization, antimicrobial and antioxidant activities. *Scientific Reports;* ***12*****(1)**:20278. https://doi.org/10.1038/s41598-022-24615-7

Naseer, M., Aslam, U., Khalid, B., & Chen, B. (2020). Green route to synthesize zinc oxide nanoparticles using leaf extracts of *Cassia fistula* and *Melia azedarach* and their antibacterial potential. *Scientific Reports;* ***10*****(1)**:9057. https://doi.org/10.1038/s41598-020-65949-3

Ologhobo, A. D., Adewale, F. A., & Lawal, O. T. (2021). Nephroprotective potentials of zinc nanoparticles in gentamicin-induced toxicity. *Biomedical Pharmacotherapy;* ***140****:* 111691. https://doi.org/10.1016/j.biopha.2021.111691

Raghupathi, K. R., Koodali, R. T., & Manna, A. C. (2011). Size-dependent bacterial growth inhibition and mechanism of antibacterial activity of ZnO nanoparticles. *Langmuir;* ***27*****(7)**: 4020–4028. https://doi.org/10.1021/la104825u

Santhoshkumar, J., Rajeshkumar, S., & Venkat Kumar, S. (2019). Phyto-mediated synthesis of zinc oxide nanoparticles using *Lannea coromandelica* leaf extract and their characterization. *Drug Invention Today;* ***11*****(12)**: 3125–3130.

Singh, P., Kim, Y. J., Zhang, D., & Yang, D. C. (2020). Green synthesis of zinc oxide nanoparticles and their biomedical applications. *Journal of Nanobiotechnology;* ***18*****(1)**: 1–15. https://doi.org/10.1186/s12951-020-00744-9

Singh, R. P., Hadiya, P. D., & Sharma, S. (2020). Zinc oxide nanoparticles: Biological synthesis and biomedical applications. *Ceramics International;* ***46*****(1)**: 123–130. https://doi.org/10.1016/j.ceramint.2019.08.272

Sirelkhatim, A., Mahmud, S., Seeni, A., Kaus, N. H. M., Hasan, H., & Mohamad, D. (2015). Review on zinc oxide nanoparticles: Antibacterial activity and toxicity mechanism. *Nano-Micro Letters;* ***7*****(3)**: 219–242. https://doi.org/10.1007/s40820-015-0040-x

Thema, F. T., Manikandan, E., Dhlamini, M. S., & Maaza, M. (2015). Green synthesis of ZnO nanoparticles via *Agathosma betulina* natural extract. *Materials Letters;* ***161****:* 124–127. https://doi.org/10.1016/j.matlet.2015.08.102

World Health Organization. (2024). *Antimicrobial resistance*. https://www.who.int/news-room/fact-sheets/detail/antimicrobial-resistance.

Yusuf, A. A., & Abubakar, B. M. (2017). Phytochemical constituents and antimicrobial activity of *Lannea subscorpioidea* Engl. & K. Krause. *Nigerian Journal of Pharmaceutical Sciences;* ***16*****(1)**: 45–52.

Yusuf, A.A., & Abubakar, M. (2017). Phytochemical screening and pharmacological potentials of *Lannea subscorpioidea*. *Journal of Ethnopharmacology;* ***206****:* 56–64. https://doi.org/10.1016/j.jep.2017.05.020

Citation: Ahmad, S.M., Abubakar A.L., Safiyya M. Shehu. Green Synthesis, Characterization, and Evaluation of Antimicrobial, Antioxidant, Hepatoprotective, and Nephrocurative Potentials of Zinc Oxide Nanoparticles Derived from *Lannea subscorpioidea (Oliv.*) Extract. ***Sokoto Journal of Medical Laboratory Science*****; 10(4): 68 – 84.** https://dx.doi.org/10.4314/sokjmls.v10i4.8